Int. J. Heat Mass Transfer. Vol. 31, No. 11, pp. 2381–2390, 1988
Printed in Great Britain

0017–9310/88 $3.00 + 0.00

A model of heat transfer in tunnel kilns used for firing refractories

D. R. DUGWELL† and D. E. OAKLEY‡
Department of Chemical Engineering, Imperial College, London SW7 2AZ, U.K.

(*Received* 31 *December* 1987 *and in final form* 26 *May* 1988)

Abstract—An improved model is presented for the prediction of gas and ware temperature profiles during the firing of refractory blocks in tunnel kilns. The model represents the kiln as a series of plug-flow regions, in which heat transfer to ware occurs, interspaced by well-stirred adiabatic regions, in which burners and air inleakages are introduced. The model is constructed in two forms differing in treatment of unsteady conduction in the ware. The two-dimensional form gives good agreement with measured ware temperature profiles. The simpler one-dimensional form predicts gas temperature profiles accurately, and estimates representative ware temperatures. Both models solve the unsteady conduction equation with strongly non-linear boundary conditions due to radiation.

INTRODUCTION

REFRACTORIES are vital to the construction of a high temperature process plant, e.g. furnaces for the metallurgical industries. Their manufacture includes a high temperature firing stage for hardening and maturation prior to service. In the modern ceramic industry, firing is usually carried out in tunnel kilns. The kilns are physically large, lengths often exceeding 100 m, aerodynamic flow patterns are complicated by multiple burners, air inleakages and the refractory ware setting (stacking) geometry.

The layout of a typical kiln is shown in Fig. 1. The ware to be fired is set on rail-mounted cars which are pushed intermittently along the kiln from field 1. Peak temperatures (up to 2070 K) are achieved in the firing zone, before the fired ware is cooled at a controlled rate by passage against incoming ambient air. Combustion is limited to the fields of the firing zone, where wall or roof mounted burners are fired into the spaces between adjacent ware settings. Exhaust gases leave the kiln at the ware input end. A cross-section of a tunnel kiln with five 'blades' of ware set on a refractory lined kiln car is shown in Fig. 2. Each car would typically, have two separate rows of five blades set on it. Each blade is idealized as a continuous rectangular block; in reality, blades are built up from stacking individual pieces of ware, which may not be linear in all dimensions. Air inleakage occurs along the length of the kiln, but particularly in the preheat section where it may be deliberately encouraged to dilute the hot exhaust gas flow.

Control of tunnel kilns has tended to rely on operator experience and empiricism because of the inherent process complexity. The firing schedule, i.e. time–temperature profile, desired for a particular refractory product is related to a regular temperature gradient along the kiln length, as measured by roof-mounted thermocouples, and to a specified car setting pattern and push rate. Kiln control is then concerned with adjusting burners and airflows to maintain the specified roof temperature profile. Traditionally, the adjustment has been manual, but newer technology employs microprocessor control of motorized valves, for fuel and air, to maintain the specified profile.

Increasing demands for tighter control of product quality and reduced operating costs, particularly fuel, require a more fundamental understanding of kiln behaviour. The kiln operator needs to be able to specify optimum process conditions in which every element of every piece of ware is exposed to the correct firing schedule, at minimum overall firing cost. The optimum condition will vary according to shape, size and composition of the ware. Determination of this optimum requires a mathematical simulation of the heat transfer processes occurring within the kiln, in order to be able to predict ware temperature distribution at all points during firing. Such a simulation will enable the operator to study the response of any refractory product to any particular set of kiln operating conditions.

Published work on tunnel kiln modelling is limited. A practical model was reported by Gardiek and Scholz [1], who assumed that the ware had a uniform temperature at each cross-section, and moved continuously. Only heat transfer between ware and gas was considered, and heat losses and air inleakage were neglected. The heating and cooling zones of the kiln approximated to a counter-current heat exchanger at steady-state, and the resultant equations could be solved analytically. The firing zone was assumed well

† Author to whom correspondence should be addressed.
‡ Now at AERE, Harwell, U.K.

NOMENCLATURE

A	area per unit length [m^2]
a	effective blade width [m]
b	blade height [m]
C	heat capacity [$J\,kg^{-1}\,K^{-1}$]
c	distance from car base to blade top surface [m]
D	blade separation [m]
d	equivalent diameter of largest cross-section of kiln [m]
E	emissive power [$W\,m^{-2}$]
F	flow rate [$kg\,s^{-1}$]
F_{jw}	configuration factor
h	coefficient of heat transfer [$W\,m^{-2}\,K^{-1}$]
J	source term in transient conduction equation [$W\,m^{-3}$]
k	thermal conductivity [$W\,m^{-1}\,K^{-1}$]
Q	heat absorbed per unit time per unit length [$W\,m^{-1}$]
q	heat flux absorbed [$W\,m^{-2}$]
T	solid temperature [K]
t	time [s]
U	kiln wall heat loss coefficient [$W\,m^{-2}\,K^{-1}$]
V	kiln car velocity [$m\,s^{-1}$]
x	Cartesian coordinate: horizontal and normal to axis [m]
y	Cartesian coordinate: vertical [m]
z	Cartesian coordinate: axial [m].

Greek symbols

α	thermal diffusivity [$m^2\,s^{-1}$]
ε	emissivity
Θ	gas temperature [K]
ρ	density [$kg\,m^{-3}$]
τ	transmissivity.

Superscripts

c	convective
p	iteration number
r	radiative.

Subscripts

a	ambient
d	deck
g	gas
i,j	increments in x-, y-directions
M	number of increments in y-direction
N	number of increments in x-direction
n	number of time step
s	surface
w	wall
0	initial state.

Dimensionless groups

Nu	Nusselt number
Pr	Prandtl number
Re	Reynolds number.

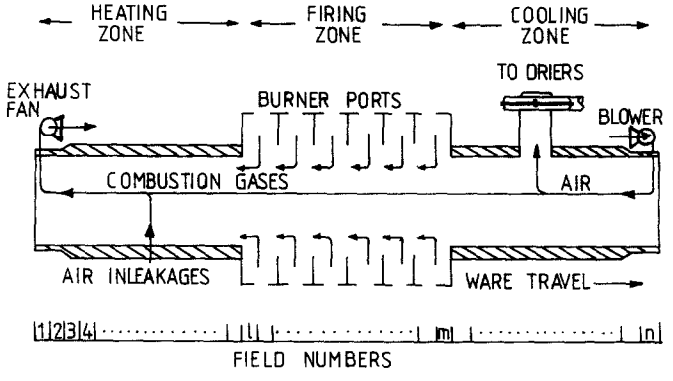

FIG. 1. Layout of typical tunnel kiln.

stirred by the burners, giving constant gas temperature in the axial direction. The model is of limited accuracy but allows for an investigation of physical principles.

Abbakumov [2] presented a model in which the blades were considered as infinite flat plates with temperature profiles governed by the one-dimensional conduction equation. Again the steady-state, continuous flow assumptions were made, and heat transfer was limited to that between ware and gas. Radiative heat transfer was approximated by a heat transfer coefficient, and after each field calculation additional considerations such as heat loss, heat absorbed by the kiln cars, and inleakages were taken into account. The model calculates the fuel requirement to each burner, and provides estimates of the gas temperature profile and ware temperature profile in one dimension and time. However, accuracy is limited, and the important, vertical temperature gradients in the ware are ignored.

The obvious scope for improvement has prompted the current work [3], resulting in a model which provides a good prediction of both ware and gas temperature profiles.

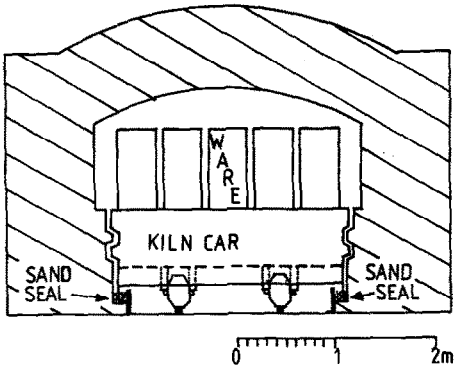

FIG. 2. Kiln cross-section showing five blades of ware set on a kiln car, and sand seals to minimize gas leakage.

PHYSICAL BASIS OF THE MODEL

The principal aim of modelling is the prediction of ware temperatures during firing. Heat is transferred between gas and ware predominantly by convection, with only a modest contribution from radiation. However, the high temperatures involved create strong radiative transfer between solid surfaces within the kiln. Heat entering the ware surface penetrates by conduction only. Provided that the combustion gases are evenly distributed around each blade, the rate of conduction within the solid governs the rate at which refractories may be fired satisfactorily [4].

Treatment of conduction

The ware and supporting kiln car, which may exceed the thermal mass of the ware, are subject to unsteady heat conduction as they traverse the kiln. The blades are represented as continuous slabs since perfect thermal contact between the constituent pieces is assumed. For an isotropic, three-dimensional solid, the process is governed by

$$\rho C\frac{\partial T}{\partial t}=\frac{\partial}{\partial x}\left(k\frac{\partial T}{\partial x}\right)+\frac{\partial}{\partial y}\left(k\frac{\partial T}{\partial y}\right)+\frac{\partial}{\partial z}\left(k\frac{\partial T}{\partial z}\right)+J \tag{1a}$$

subject to the initial conditions

$$T(x,y,z,t=0)=T_0(x,y,z) \tag{1b}$$

and the boundary condition of either specified surface temperature

$$T_s=f(x,y,z,t) \tag{1c}$$

or heat flux

$$\frac{\mathrm{d}T_s}{\mathrm{d}n_i}=f(x,y,z,t) \tag{1d}$$

where $\mathrm{d}/\mathrm{d}n$ indicates differentiation outward and normal to the surface. The heats of the reactions for the changes taking place during firing have been estimated by McColm [5] for a clay-based ceramic material. The combined contributions from sintering (4 kJ kg^{-1}), production of a 5% liquid phase (15 kJ kg^{-1}), and solid state transformations (40 kJ kg^{-1}) are far outweighed by the sensible heat requirement for firing to 1770 K (1200 kJ kg^{-1}). It has been assumed therefore that J may be neglected. Similarly, since the physical properties, k, ρ, C of fired refractory materials vary only weakly with temperature, the thermal diffusivity may be taken as a constant, allowing equation (1a) to be written in the form

$$\frac{\partial T}{\partial t}=\alpha\left[\frac{\partial^2 T}{\partial x^2}+\frac{\partial^2 T}{\partial y^2}+\frac{\partial^2 T}{\partial z^2}\right]. \tag{2}$$

The equation may be further reduced to two dimensions only, by disregarding conduction in the axial direction. The relatively minor variation in surface temperature along the axis of a blade, compared to the surface to centre variation provides justification for this assumption.

This treatment is acceptable in the central portion of a blade where the influence of axial conduction from the end faces is negligible. However, for the heat transferred into the ware and the heat transferred from the gas to be consistent, the end faces must be assumed unavailable for heat transfer. The two-dimensional treatment of conduction therefore approximates a real blade as a rectangular parallelepiped with insulated end faces.

A simpler version of the model solves the conduction equation in one dimension only, i.e. laterally into the ware, whilst the two-dimensional version provides for analysis in the vertical direction also. The unsteady conduction equation is solved in the one-dimensional solid bounded by parallel planes separated by a, the effective thickness of the blade

$$a=\frac{2\times\text{volume of blade}}{\text{surface area of blade}}$$

so that the volume : surface ratio is identical to the original blade. This treatment is much less conservative than the two-dimensional treatment of conduction since the effective thickness will always be less than the smallest dimension of a blade.

In both cases the ware moves steadily through the kiln and, therefore, axial displacement, z, and time within the kiln, t, are related by

$$z=Vt.$$

Treatment of convection

Forced convection is the dominant mode of heat transfer from the gas, especially in the heating and cooling zones where the gas phase has a low emissivity.

Experiments have been conducted on a laboratory model in order to provide estimates of convective heat transfer coefficients, since direct measurements on a working kiln are impracticable. A 1/10 scale model of a section of a production kiln was constructed through which heated air was passed. The model provided for geometric similarity, and also for acceptable dynamic similarity [6], with Reynolds numbers of around 20 000. Convective heat transfer coefficient estimates

were derived from measurements of heat fluxes by heat flow meters stuck to the faces of the chrome magnesite blocks used to simulate the blades of the real kiln. Data were correlated in the form

$$Nu = f(Re, Pr, D/d).$$

Generally, heat transfer coefficients to side, top, and front faces of blades are found to be of the same order, whilst those to the back faces are perhaps 50% lower. Increasing blade separation, tends to reduce heat transfer. Actual values of the heat transfer coefficient measured ranged from 36.0 ± 1.0 to 100.8 ± 4.3 W m^{-2} K^{-1}.

Convective heat transfer has been incorporated into the model by a series of heat flow/flux expressions. In the case of the one-dimensional model

$$q^c = h(\Theta - T_s). \tag{3a}$$

In the two-dimensional model allowance must be made for heat exchange into horizontal as well as vertical faces (Fig. 3)

$$q1(x)^c = h_{top}(\Theta - T(x, 0)) \tag{3b}$$

$$q2(y)^c = h_{side}(\Theta - T(0, y)) \tag{3c}$$

$$q3(x)^c = h_{bottom}(\Theta - T(x, b)) \tag{3d}$$

$$Q_w^c = h_w A_w(\Theta - T_w). \tag{3e}$$

Treatment of radiation

The radiation exchange within the kiln is determined by a simple zone method. Fortunately the geometry of a typical tunnel kiln facilitates the neglection of axial radiative transfer since this allows a marching method of solution to be adopted. The gas phase temperature is assumed constant at each cross-section and all surfaces are black.

In the one-dimensional model the radiative exchange is between the gas, the kiln wall and one surface representing the ware. In the two-dimensional model the ware surface is divided into incremental areas.

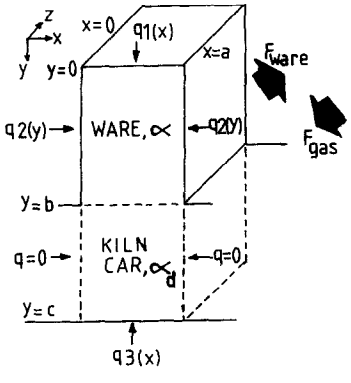

FIG. 3. Representation of heat flows into the ware and kiln car for the two-dimensional model.

In the two-dimensional model (Fig. 4) for an element i on the blade top surface

$$q_i^r = E_w\tau_{wi} + \varepsilon_g E_g - E_i. \tag{4a}$$

A surface element j on the blade side receives much less radiation since it only views the kiln wall as a narrow strip. The adjacent blade surface is assumed to be at nearly the same temperature as j and therefore there is negligible net radiative heat transfer between them

$$q_j^r = F_{jw}(E_w\tau_{wj} + \varepsilon_g E_g - E_j). \tag{4b}$$

The configuration factor F_{jw} is calculated from an exact formula [7]. The radiative properties of the gas, i.e. τ_{wi}, τ_{wj}, ε_g are calculated from the empirical correlations of Hadvig [8] fitted to the data of Hottel [9].

Treatment of ware movement. The intermittent pushing of the kiln cars is approximated by steady motion. Analysis of kiln wall thermocouple response to pushing indicates that this approximation introduces little error. After an initial drop of around 100 K, recovery to the local steady-state condition occurs within a period of 15 min which is short in comparison with the pushing interval of 5 h, or more. High thermal inertia of the walls, and predominance of radiant exchange permits this prompt temperature equalization.

Treatment of gas flow. Two major assumptions have been made in treating the kiln gas. The flow has been considered in the axial direction only, and gas temperature and composition have been considered uniform at each cross-section. The first assumption is suggested by the dimensions of the kiln and the linear setting patterns of the ware, and can be justified by observations made on production kilns.

The assumption of cross-sectional uniformity is suggested by the combination of the natural mechanics of turbulence and convection. The natural tendency to thermal stratification due to buoyancy, with hotter gas collecting in the roof arch, is countered by the vigorous mixing effect of burners and of roof-mounted artificial mixing devices. Burners, firing perpendicular to the main gas flow, are mounted either on alternate sides of the kiln, or opposed, but at different heights, on the same cross-section to induce swirl. Detailed measurements on production kilns indicate that this second assumption is justified, since temperature and composition profiles across the kiln tend to be flat except in the regions immediately adjacent to the kiln wall.

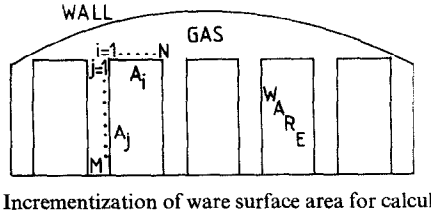

FIG. 4. Incrementization of ware surface area for calculation of radiant heat exchange in the two-dimensional model.

Treatment of combustion and air inleakage

The predominant use of natural gas in well-aerated premixed flames in modern tunnel kilns renders detailed consideration of the combustion process unnecessary. Flames are essentially non-luminous so that burners provide only an input of heat, and momentum to induce mixing, in the gaps between adjacent cars. They do not introduce intense radiation sources in close proximity to the blade ends. It is therefore permissible to consider the burners as an input of hot combustion gases which mix immediately with the kiln gas flow without transferring any heat to the ware.

Air inleakage occurs at various points in the kiln with the major part being induced deliberately for dilution purposes. Local inleakage rates can be related to operating conditions on particular kilns. The inleakages are treated in a similar manner to flames, i.e. by local adiabatic mixing with kiln gases.

The gas temperature, flow rate and composition after burners and inleakages are calculated by simple mass and energy balances.

Treatment of heat losses

Between 5 and 10% of total thermal input to a kiln will be lost through the kiln structure. Detailed measurement of kiln wall and surface temperature distributions may be used to calculate the total heat loss from each field of a particular kiln. The measured heat loss distribution can then be input into a simulation of that kiln.

THE SOLUTION PROCEDURE

The idealization of the kiln as a continuous process operating at steady state, and the introduction of burners and inleakages as discrete energy and mass inputs into the gas stream, leads to the kiln being represented as a series of plug-flow regions interspaced by well-stirred adiabatic regions. In the well-stirred regions new gas flow rates and temperatures are calculated from mass and energy balances. In the plug-flow regions gas and solid temperatures are governed by differential equations: for gas temperature (z-direction against gas flow)

$$\frac{\mathrm{d}\Theta}{\mathrm{d}z} = \frac{-Q_g}{F_g C_g} \tag{5a}$$

$$\Theta(L) = \Theta_a \tag{5b}$$

for ware temperatures

$$L[T] = 0 \tag{6a}$$

$$T(t = 0) = T_0 \tag{6b}$$

where the operator L represents:

(i) in the case of the one-dimensional model

$$L[T] = \frac{\partial T}{\partial t} - \alpha \frac{\partial^2 T}{\partial x^2}; \tag{6c}$$

(ii) in the case of the two-dimensional model

$$L(T) = \frac{\partial T}{\partial t} - \alpha \frac{\partial^2 T}{\partial x^2} - \alpha \frac{\partial^2 T}{\partial y^2} \tag{6d}$$

with specified heat flux boundary conditions in both cases.

These equations must be solved in conjunction with the convective and radiative transfer equations of the preceding section. The operator L, is parabolic creating a marching problem, i.e. the solution marches out from the initial state, guided and modified by the boundary conditions as they are encountered. Since $\Theta(L)$ and T_0 are specified at opposite ends of the kiln the model is a boundary value problem also.

It may be noted that if unsteady conduction in the ware is modelled in three dimensions, the third spatial derivate $\partial^2 T/\partial z^2$ is introduced, and the equation becomes elliptical. Solution will then depend on the boundary conditions at forward time (or z) steps which would have to be satisfied simultaneously.

The numerical methods must obey the condition of absolute stability so that the effect of rounding and truncation errors does not increase at subsequent time steps. This has led to the selection of implicit rather than explicit methods here. In addition attention must be paid to the mesh size (Δx and Δy) in order to avoid problems of stiffness.

The problem of inherent instability would be encountered over large regions of the kiln if calculation of the ware temperature proceeded with the gas flow. However, this problem is avoided by performing calculations against the gas flow. The choice of calculation against the flow is also desirable because the unknown ware profiles at the cooling zone end of the kiln represent more unknowns than the unspecified exhaust temperature at the heating zone end.

Numerical solution of the unsteady conduction equation has been achieved by the well-known finite difference methods of Crank and Nicolson [10] for the one-dimensional case, and of Peaceman and Rachford [11], the alternating direction implicit (ADI) method, for the two-dimensional case. Since the equations for gas and ware temperatures must be solved in parallel, and the boundary conditions are nonlinear here, these methods have had to be used in conjunction with an iterative procedure to calculate heat transfer at a forward time step (i.e. a predictor–corrector method).

Solution of the one-dimensional model plug-flow region

Equations (11) and (12) govern temperatures in the one-dimensional model, with boundary conditions

$$\text{at } x = 0, \quad \frac{\partial T}{\partial x} = \frac{-q(\Theta, T)}{\alpha} \tag{7a}$$

$$\text{at } x = a, \quad \frac{\partial T}{\partial x} = q\frac{(\Theta, T)}{\alpha} \tag{7b}$$

Q_g and q are non-linear functions of gas and ware surface temperatures.

The kiln is divided into a number of increments of length Δz in the axial direction and the ware is divided into strips of thickness Δx in a lateral direction (Fig. 5).

The unsteady conduction equation is approximated by the well-known Crank–Nicolson scheme

$$T_{i,n+1}-T_{i,n}=\frac{r}{2}(T_{i-1,n}-2T_{i,n}+T_{i+1,n})+\frac{r}{2}(T_{i-1,n+1}-2T_{i,n+1}+T_{i+1,n+1}) \quad (8a)$$

where

$$r=\alpha\Delta t/(\Delta x)^2.$$

Rearranging with unknowns on the left

$$-rT_{i-1,n+1}+(2+2r)T_{i,n+1}-rT_{i+1,n}=rT_{i-1,n}+(2-2r)T_{i,n}+rT_{i+1,n}. \quad (8b)$$

The specified heat flux boundary conditions are approximated by introducing fictitious external temperatures $T_{0,n}$ and $T_{N+1,n}$ such that

$$T_{0,n}=T_{2,n}+2\Delta xq_n/\alpha \quad (9a)$$

$$T_{N+1,n}=T_{N-1,n}+2\Delta xq_n/\alpha \quad (9b)$$

where in general q_n, the heat flux absorbed at time step n is a non-linear function of Θ and T_s. Inserting equation (9a) into equation (8b), at $i=1$

$$(2+2r)T_{1,n+1}-2rT_{2,n+1}-2r\Delta xq_{n+1}/\alpha=(2-2r)T_{1,n}+2rT_{2,n}+2r\Delta xq_n/\alpha \quad (9c)$$

similarly, at $i=N$.

The system of algebraic equations (9), for $i=1$–N, can be written in matrix notation as

$$\mathbf{AT}_{n+1}-\mathbf{F}_{n+1}=\mathbf{BT}_n+\mathbf{F}_n \quad (10a)$$

where

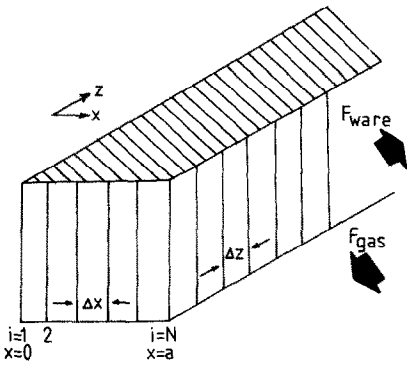

FIG. 5. Incrementization of ware for calculation of transient conduction in the one-dimensional model.

$$\mathbf{A}=\begin{vmatrix}2+2r & -2r & & \\ -r & 2+2r & -r & \\ & -r & 2+2r & -r\end{vmatrix} \quad (10b)$$

$$\mathbf{B}=\begin{vmatrix}2-2r & 2r & & \\ r & 2-2r & r & \\ & r & 2-2r & r\end{vmatrix} \quad (10c)$$

and

$$\mathbf{F}_n=2r\frac{\Delta x}{\alpha}[q_n,0,\ldots,0,q_n]^{\mathrm{T}} \quad (10d)$$

hence

$$\mathbf{T}_{n+1}=\mathbf{A}^{-1}(\mathbf{BT}_n+\mathbf{F}_n+\mathbf{F}_{n+1}). \quad (11)$$

Since $\mathbf{A}$ is a tridiagonal matrix it can be inverted directly by the Thomas algorithm, a process similar to Gaussian elimination. $\mathbf{F}_{n+1}$ must be found by iteration.

The differential equation governing gas temperature (5a) is solved by the trapezoidal method

$$\Theta_{n+1}=\Theta_n+\Delta z(\Theta'_n+\Theta'_{n+1})/2 \quad (12)$$

where $\Theta'=-Q_g/F_gC_g$, Q_g, being a non-linear function generally, must be found by an iterative procedure.

The equations governing heat transfer between gas and solid surfaces require a value of the temperature of the wall, in addition to that of the ware surface and adjacent gas. The value of T_w is determined by bisection from

$$F(T_w)=A_wU(T_w-\Theta_a)-Q_w=0 \quad (13)$$

T_w must lie between either Θ and Θ_a, or T_s and Θ_a.

The solution then proceeds by calculation of the functions $\mathbf{F}_{n+1}$ and g_{n+1} at a forward time step by the prediction–correction procedure ($g=\Delta z\Theta'$).

Prediction is provided by

$$\mathbf{AT}^1_{n+1}=\mathbf{BT}_n+2\mathbf{F}_n \quad (14a)$$

$$\Theta^1_{n+1}=\Theta_n+g_n. \quad (14b)$$

Correction is provided by

$$\mathbf{AT}^{p+1}_{n+1}=\mathbf{BT}_n+\mathbf{F}_n+\mathbf{F}^p_{n+1} \quad (15a)$$

$$\Theta^{p+1}_{n+1}=\Theta_n+(g_n+g^p_{n+1})/2. \quad (15b)$$

Temperature calculation proceeds from unknown values at the nth time step, through predicted values at the $n+1$th step, to calculated values at the $n+1$th step (by the Thomas algorithm). Correction of the values at the $n+1$th step are applied and the process repeated until $|T^{p+1}_{n+1}-T^p_{n+1}|$ is less than the specified error.

Solution of the two-dimensional model of plug-flow region

Visualization of this region has been provided in Fig. 3, and also in Fig. 4. The gas temperature is governed by equation (5a).

Ware temperatures are governed by the two-dimensional conduction equation for the ware

$$\frac{\partial T}{\partial t} = \alpha\left(\frac{\partial^2 T}{\partial x^2} + \frac{\partial^2 T}{\partial y^2}\right) \tag{16a}$$

and for the kiln car

$$\frac{\partial T}{\partial t} = \alpha_d\left(\frac{\partial^2 T}{\partial x^2} + \frac{\partial^2 T}{\partial y^2}\right) \tag{16b}$$

with initial conditions

$$T(x, y, 0) = T_0(x, y) \tag{16c}$$

and boundary conditions

$$\text{at } y = 0, \quad \frac{\partial T}{\partial y} = \frac{-q1(x)}{\alpha} \tag{16d}$$

$$\text{at } y = c, \quad \frac{\partial T}{\partial y} = \frac{q3(x)}{\alpha_d} \tag{16e}$$

$$\text{at } x = 0, y \leqslant b, \quad \frac{\partial T}{\partial x} = \frac{-q2(y)}{\alpha} \tag{16f}$$

$$\text{at } x = a, y \leqslant b, \quad \frac{\partial T}{\partial x} = \frac{-q2(y)}{\alpha} \tag{16g}$$

$$\text{at } x = 0 \text{ or } a, y > b, \quad \frac{\partial T}{\partial x} = 0. \tag{16h}$$

This system of equations is solved using the ADI method whereby the value of one of the two second-order derivatives is supplied by implicit approximation, the other by explicit approximation. In the first time step $\partial^2 T/\partial x^2$ is approximated implicitly, resulting in $(M-2)$ independent systems of equations, each system consisting of $(N-2)$ equations in tridiagonal form. Then in the second time step $\partial^2 T/\partial y^2$ is approximated implicitly, resulting in $(N-2)$ independent systems of $(M-2)$ equations in tridiagonal form. The Thomas algorithm is used to solve the tridiagonal matrix in both cases. Each step on its own is unstable, but the ADI approximations produce overall unconditional stability over the double time steps.

The boundary conditions are again of the prescribed heat flux type, and are approximated using the fictitious external temperature concept used in the one-dimensional model.

Strictly speaking, at the interface between the kiln and the ware the condition

$$\alpha\frac{\partial T}{\partial y} = \alpha_d\frac{\partial T_d}{\partial y} \tag{17a}$$

applies. Fortunately, it is acceptable to treat the interface merely as a region of variable conductivity. Unsteady conduction then obeys

$$\rho C\frac{\partial T}{\partial t} = \frac{\partial}{\partial y}\left(\alpha\frac{\partial T}{\partial y}\right) + \frac{\partial}{\partial x}\left(\alpha\frac{\partial T}{\partial x}\right). \tag{17b}$$

This implies condition (17a) since otherwise $(\partial/\partial y)(\alpha(\partial T/\partial y))$ will be infinite and hence $\rho C(\partial T/\partial t)$ will be infinite towards a temperature which satisfies equation (17a).

The modelling scheme may be written in matrix form for the nth time step

$$\mathbf{A1}\,\mathbf{T1}_{n+1} + \mathbf{F1}_{n+1} = \mathbf{B1}\,\mathbf{T1}_n + \mathbf{G1}_n \tag{18a}$$

and the $n+1$th time step

$$\mathbf{A2}\,\mathbf{T1}_{n+2} + \mathbf{F2}_{n+2} = \mathbf{B2}\,\mathbf{T2}_{n+1} + \mathbf{G2}_{n+1} \tag{18b}$$

where **A1** and **A2** are the tridiagonal matrices. Both $\mathbf{T1}_n$ and $\mathbf{T2}_n$ are vectors of temperatures at the nth time step taken row by row, and column by column, respectively.

The column matrices **F1** and **F2** represent implicitly calculated boundary conditions; $\partial T/\partial x$ taken row by row, and $\partial T/\partial y$ taken column by column, respectively.

The column matrices **G1** and **G2** represent explicitly calculated boundary conditions; $\partial T/\partial y$ taken row by row, and $\partial T/\partial x$ taken column by column, respectively.

For each double time step used in the ADI method the gas temperature is calculated in a single step using the trapezoidal rule

$$\Theta_{n+2} = \Theta_n - 2\Delta z Q_{g,n+1}/F_g C_g \tag{19a}$$

where

$$Q_{g,n+1} = (Q_{g,n} + Q_{g,n+2})/2. \tag{19b}$$

The value of wall temperature, T_w, necessary for solution of the heat transfer equation is found by bisection from

$$F(T_w) = A_w U(T_w - \Theta_a) - Q_w = 0. \tag{20}$$

A prediction–correction procedure, similar to the one-dimensional model, is used to permit solution of the overall system of equations.

Solution proceeds from known temperatures at the nth step, through predicted temperatures at the $n+1$th and $n+2$th step, via the correction procedure, to acceptable values at the next time step.

Well-stirred regions

When a burner or inleakage is encountered the new gas mass flow rates and enthalpy are calculated by the Newton–Raphson method. The new values are then fed to the next plug-flow region calculation.

Overall solution scheme and the boundary value problem

Integration against the gas flow means that the exhaust gas temperature, $\Theta(0)$, is unknown initially. Solution is accomplished by a shooting method whereby two initial estimates of $\Theta(0)$ are made, the complete system of plug flow and well-stirred regions calculated, and the resultant values of gas inlet (ambient air at the cooling end of the kiln) temperatures are compared with the desired value.

New estimates of $\Theta(0)$ are generated, and the process repeated until the estimated gas inlet temperatures become sufficiently close to the desired value.

MATHEMATICAL MODEL PERFORMANCE

The model has been tested by comparison against data from a production kiln of Steetley Refractories Limited (Worksop, Nottinghamshire).

An indication of the potential of the models is given diagrammatically in Figs. 6–10. The first diagram, Fig. 6, gives a comparison of the predicted gas temperature profiles for both versions of the model for one particular kiln operating condition. There is a clear disparity between the two profiles, particularly in the firing and cooling zones. Peak temperatures predicted are, 2003 K in field 17 (one-dimensional) and 1924 K in field 17 (two-dimensional). The step nature of the curves in the heating and firing zone is a function of the calculation procedure moving between plug flow and adiabatic mixing regions. The sharp change of slope in field 32 of the cooling zone coincides with the removal of air to the driers, whilst the smaller perturbation in field 23 corresponds to the introduction of combustion air. Introduction of fuel creates a sharp transition between the firing and cooling zones.

Figure 7 compares kiln wall temperature profiles. The comparison is between the kiln operating limits, actual kiln measurements, and the one-dimensional model prediction at two different airflows; that measured, and at a reduced rate and lower fuel rate (by 15%). The prediction matches plant data well at the

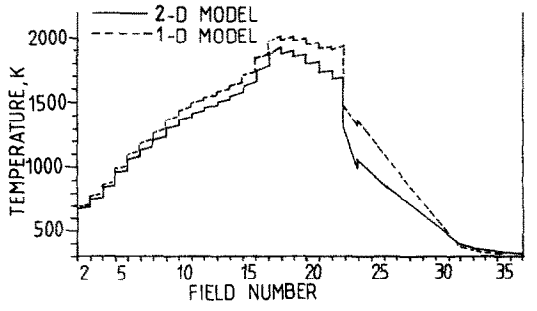

FIG. 6. Gas temperature profile: comparison between the predictions of the one- and two-dimensional models for one kiln operating condition.

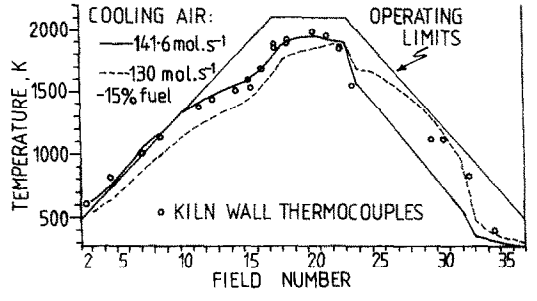

FIG. 7. Kiln wall temperature profiles: comparison between the one-dimensional model prediction, plant measurements, and kiln design operating limits.

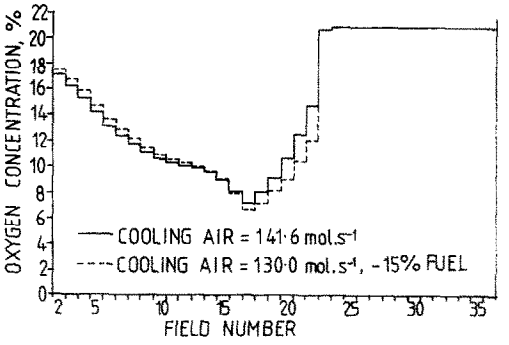

FIG. 8. Oxygen concentration profiles: comparison between the predictions of the one-dimensional model at two different cooling air and fuel flow rates.

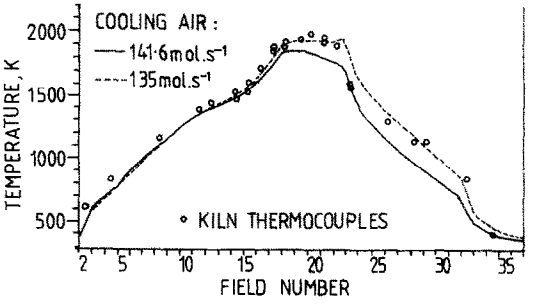

FIG. 9. Ware surface temperature profiles: comparison between the predictions of the two-dimensional model at two different cooling air and fuel flow rates, and plant measurements.

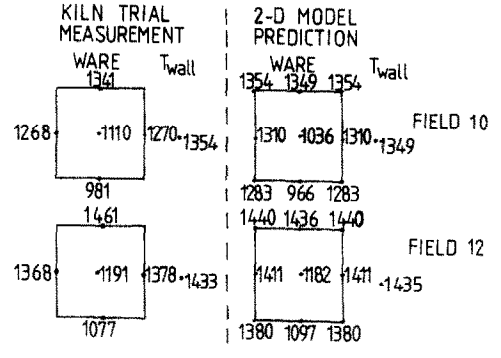

FIG. 10. Temperature distribution around ware in fields 10 and 12 for one kiln operating condition: comparison between the prediction of the two-dimensional model and plant measurements.

actual flow rate in the heating and firing zones, although better matching is achieved at the lower flow rate towards the cold end of the kiln. However, at the kiln outlet the predicted temperatures converge. This figure demonstrates the accuracy of the one-dimensional model in predicting kiln wall temperatures in the heating and firing zone, and also suggests the potential of the model for determining better operating conditions with regards to fuel consumption and safeguarding of kiln linings.

Figure 8 shows a prediction of the oxygen concentration profile for the one-dimensional model under the same conditions as in Fig. 7. Air enters the

kiln at the cold end, and is subsequently diluted by fuel to a minimum oxygen concentration of around 7% in the firing zone. Air inleakages increase oxygen concentration thereafter. Similar profiles can be generated for other gaseous species.

Figures 9 and 10 demonstrate the potential of the two-dimensional model for predicting ware temperature profiles. Figure 9 compares plant measurement of ware surface temperature with predictions of the model at two airflows. The quality of prediction is shown to be very sensitive to the airflow used, which is a measurement subject to some error given the huge flows involved on the production plant. The measured airflow prediction gives excellent agreement in the heating zone, with some divergence thereafter. However, a near perfect match along the whole kiln length is achieved with an airflow reduced by 4.7%.

Figure 10 compares local temperatures, derived from an instrumented kiln car, with the model predictions, at two field locations within the heating zone, for one particular test condition. It can be seen that the kiln wall temperatures predicted by the model coincide almost exactly with the plant measurement. Furthermore, the temperatures predicted for the blade surfaces (top, side and base) and centre are in good agreement with the plant data, given the uncertainty of locating individual thermocouple tips in the experiment. Although correspondence is not perfect, the prediction of trends in temperature differences around the blade is particularly instructive, highlighting a measured maximum difference, between top centre, and base centre of over 330 K in each case.

CONCLUSIONS

(1) A model has been developed to simulate the firing of refractories in natural gas fired tunnel kilns. The model considers the kiln as a series of plug-flow regions, in which heat is transferred between kiln gases and the ware, and well-stirred adiabatic regions, in which mass inputs of fuel or inleaking air occur.

(2) Heat transfer into or out of, the ware, in the plug-flow regions, is limited by unsteady conduction. The model includes two options for considering this unsteady conduction. A one-dimensional treatment of the unsteady conduction, employing the method of Crank and Nicolson, leads to a time-dependent simulation in the one-dimensional space of the kiln. A two-dimensional treatment of the unsteady conduction, employing the ADI method of Peaceman and Rachford, leads to a time-dependent simulation in two-dimensional space of the kiln. Use of the former option, which requires less computing time, is limited to situations where accurate prediction of the ware internal temperature distribution is not sought.

(3) Comparison with production plant data demonstrates the potential of the one-dimensional version of the model for prediction of gas and kiln wall temperature, and gas composition profiles along the kiln.

(4) Comparison with production plant data demonstrate the potential of the two-dimensional version of the model for predicting the temperature distribution within the ware as it traverses the kiln.

(5) The model has been developed as an aid to improved refractory tunnel kiln operation, and may be used for kiln optimization, investigation of occasional firing problems, and for establishing desirable firing conditions for new products. Financial benefits may accrue from increased product throughput, reduction in firing rejects, reduced specific fuel consumption, and improved kiln lining life.

Acknowledgements—The authors would like to acknowledge the financial support of the Science and Engineering Research Council, and of Steetley Refractories Limited, Worksop, Nottinghamshire, U.K., to one of us (D.E.O.), and Steetley's overall support of the project including provision of plant data. Particular thanks are due here to Dr I. K. Smithson.

REFERENCES

1. H. O. Gardiek and R. Scholz, Thermal technology for tunnel kiln firing in the ceramic industry, *Interceram.* **30,** 4–6 (1981).
2. V. G. Abbakumov, Analysing the heating and cooling of products in a high temperature tunnel kiln, *Refractories* **9**(2), 77–82 (1968).
3. D. E. Oakley, Simulation of tunnel kilns for firing refractory products, Ph.D. thesis, Imperial College, University of London (1986).
4. F. H. Norton, *Refractories*, 4th Edn, Chap. 13. McGraw-Hill, New York (1968).
5. I. J. McColm, *Ceramic Science for Material Technologists*. Leonard-Hill, Glasgow (1981).
6. R. E. Johnstone and M. W. Thring, *Pilot Plant, Models and Scale-up in Chemical Engineering*, Chap. 3. McGraw-Hill, New York (1957).
7. R. Siegel and J. R. Howell, *Thermal Radiation Heat Transfer*, 2nd Edn. Hemisphere, London (1981).
8. S. Hadvig, Gas emissivity and absorptivity; a thermodynamic study, *J. Inst. Fuel* **43,** 129–135 (1970).
9. H. C. Hottel, *Heat Transmission* (Edited by W. H. McAdams), 3rd Edn, Chap. 4. McGraw-Hill, New York (1954).
10. J. Crank and P. Nicolson, Solutions of partial differential equations of the heat conduction type, *Proc. Camb. Phil. Soc.* **43,** 50–67 (1947).
11. D. W. Peaceman and H. H. Rachford, The numerical solution of parabolic and elliptical differential equations, *J. Soc. Ind. Appl. Math.* **3,** 28–41 (1955).

UN MODELE DE TRANSFERT DE CHALEUR DANS DES FOURS UTILISE POUR LE CHAUFFAGE DES REFRACTAIRES

Résumé—Presentation d'un modèle avancé pour la prediction des profils de température du gaz et de l'élément pendant le chauffage de blocs réfractaires dans des fours. Le modèle représente le four comme une série d'éléments invariables où le transfert de chaleur apparaît, alternativement séparés par des régions adiabatiques et uniformes où les brûleurs et les arrivées d'air sont introduits. Le modèle est conçu en deux parties qui diffèrent dans le traitement de conduction instable dans l'élément. La forme di-dimensionnelle correspond bien aux profils de température mesurés pour les éléments. La plus simple des formes une-dimensionnelle prédit exactement les profils de température du gaz et donne une estimation des températures représentatives de l'élément. Les deux modèles donnent une solution à l'équation de conduction instable avec des conditions limites non linéaires qui sont dues au phénomène de radiation.

EIN MODELL DER WÄRMELEITUNG IN TUNNELBRENNÖFEN ZUM BRENNEN VON FEUERFESTEN BLÖCKEN

Zusammenfassung—Präsentiert wird ein verbessertes Modell für die Voraussage von Gas- und Gut-Temperaturprofilen während des Brennens von feuerfesten Blöcken in Tunnelbrennöfen. Das Modell stellt den Brennöfen als eine Reihe von Gebieten dar, wobei sich Gebiete mit Pfropfenströmung, in denen der Wärmeübergang stattfindet, mit adiabatischen, gut durchmischten Gebieten, in denen Brennen und Luftzutritte behandelt werden, abwechseln. Das Modell ist in zwei Formen, die sich in der Behandlung der unstetigen Leitung im Gut unterscheiden, aufgebant. Die 2-dimensionale Form liefert gute Übereinstimmung mit gemessenen Guttemperaturprofilen. Die einfachere 1-dimensionale Form liefert exakte Voraussage der Gastemperaturprofile und schätzt repräsentative Guttemperaturen ab. Beide Modelle lösen die unstetige Leitungsgleichung mit stark nicht-linearen Grenzbedingungen aufgrund von Strahlung.

МОДЕЛЬ ТЕПЛОПЕРЕНОСА В ПЕЧАХ ТУННЕЛЬНОГО ТИПА, ИСПОЛЬЗУЕМЫХ ДЛЯ ОБЖИГА ОГНЕУПОРОВ

Аннотация—Предложена улучшенная модель для расчета профилей температуры в газе и в изделиях при обжиге огнеупорных блоков в печах туннельного типа. Печь моделируется рядом областей со стержневым режимом течения, в которых происходит перенос тепла к изделию, перемежающихся с зонами хорошо перемешанных адиабатических течений, в которые введены горелки и где происходит подсос воздуха. Предложены две модели, отличающиеся описанием нестационарной теплопроводности в изделии. Двумерная модель дает хорошее совпадение с измеренными температурными профилями изделий. Более простая одномерная форма дает точные значения температурных профилей в газе и достоверную оценку температуры изделий. В обеих моделях решается нестационарное уравнение теплопроводности при сильно нелинейных граничных условиях, обусловленных излучением.